IEEE Access
Multidisciplinary | Rapid Review | Open Access Journal

Received October 7, 2021, accepted October 28, 2021, date of publication October 29, 2021, date of current version November 8, 2021.

Digital Object Identifier 10.1109/ACCESS.2021.3124334

Adaptive Super-Twisting Distributed Formation Control of Multi-Quadrotor Under External Disturbance

CHENG ZHANG[1], TIANLONG CHEN[2], WEI SHANG[2], ZHONGZHONG ZHENG[2], AND HUIZHENG YUAN[1]

[1]School of Innovative Education, Hubei University of Technology (HBUT), Wuhan 430068, China
[2]School of Mechanical Engineering, Hubei University of Technology (HBUT), Wuhan 430068, China

Corresponding author: Wei Shang (bitshw@126.com)

This work was supported by the Collaborative Innovation Center of Intelligent Green Manufacturing Technology and Equipment, Shandong, under Grant IGSD-2020-007.

ABSTRACT In this paper, the adaptive super-twisting distributed formation control of multi-quadrotor in the presence of external disturbances and uncertainties is studied. First, the quadrotor formation system is separated into a position subsystem and an attitude subsystem which are represented by unit-quaternions. And then a composite adaptive super-twisting control method is proposed for the position subsystem and attitude subsystem respectively. For the position subsystem, an adaptive multivariable super-twisting controller is designed such that the positions of formation converge to the desired formation configuration and generate the desired attitude. And the adaptive fast super-twisting controller is designed for the attitude subsystem to track the desired attitude in finite time. Based on Lyapunov-based stability analysis, finite time convergence stability of the whole closed-loop system is proved. Finally, a numerical simulation result is provided to illustrate the effectiveness of the proposed formation control scheme.

INDEX TERMS Formation control, finite time convergence, quadrotor, adaptive super-twisting control, disturbance.

I. INTRODUCTION

In recent years, the quadrotor control problem has received much interest from many researchers. The main reason is the diversity of quadrotor applications, such as geographic survey, agricultural plant protection, military reconnaissance and so on [1]–[5]. However, due to its characteristics including that nonlinear, strong coupling multi-variable, under-actuated and so on, it puts forward high requirements for its control ability. The quality of control performance greatly affects the safety and stability of quadrotor.

Compared with a single quadrotor, the quadrotor formation may provide a better performance for the difficult tasks [6]–[10]. Furthermore, system stability and reliability can also be improved through the exchange of information among multiple quadrotors. Meanwhile, formation control of quadrotor formation is more challenging. And the main issue of formation control is how to achieve and maintain the desired configuration while tracking a desired trajectory. Hence, it is practical significance to study the formation control problem for quadrotors [11].

For achieving the formation control, the typical control strategies can be categorized as leader-follower [12]–[14], behavior-based [15] and virtual [16], [17]. These strategies all lack their own drawbacks [18]. However, for the reason of simplicity and flexibility of leader-follower strategy, this strategy is the most widely employed and most efficient approach for quadrotor formation control. Meanwhile, to avoid the formation falling caused by the failure of the leader, leader-follower strategy is integrated with distributed formation control approach, which is more suitable for a large number of quadrotors to maintain the formation configures. And a great deal of literature has been presented for the formation control problem by this strategy.

For the leader-follower formation problem of quadrotors, Jasim and Gu [19] developed a suboptimal H-infinity controller. However, this paper is only expected to perform a formation flight in the x-y plane and use a PID control law to control the inner-loop, which may lead to a poor control performance. Liu *et al.* [20] proposed a robust formation control

The associate editor coordinating the review of this manuscript and approving it for publication was Huiqing Wen.

based on backstepping approach for a group of quadrotors. The convergence performance is not discussed in this paper. A consensus formation control algorithm is also proposed and utilized in [21], the inner-loop modeled by quaternion can be stable in finite time, but the outer-loop is not. Du *et al.* [22] presented a finite-time formation control algorithm in the basis of backstepping approach and the finite time convergence characteristic is proved in outer-loop and inner-loop respectively, but the finite time convergence of closed system is not discussed. In addition to the above methods, the optimal control method is also used in the formation control problem of quadrotor. In [23], a formation control algorithm was proposed based on optimal control method, which aims to achieve the desired formation behaviors of multiple quadrotors in asymptotic stability with not finite time stability. Although the above methods improve the control performance to a certain extent, the further improvement performance is urgently needed, especially the convergence rate.

Over the years, sliding mode control has been applied into many nonlinear robust control systems because of its insensitivity to matched disturbances and finite time convergence [24]–[28]. However, many sliding mode controllers have the problem of chattering, and then the second order sliding mode control is developed. It can hide the switching terms within the derivatives of the controllers themselves. In addition, the super-twisting algorithm has been immensely popular since its inception [29]–[32]. Recently, there has been a lot of interest in adaptive versions of the super-twisting algorithm [33], [34]. The adaptive law can change the control gain. When a second order sliding surface is established, the adaptive law stops and the gain remains constant. One advantage of this adaptive method is that the boundary information of the disturbance can be unknown. However, for the characteristics of quadrotor formation system mentioned above, there are so many problems that need to be considered in the application of this algorithm, such as external interference, communication between quadrotors, the selection of adaptive parameters and so on. These problems increase the difficulty of applying this method to multi-quadrotors. And this paper considers a multivariable adaptive super-twisting sliding mode control method for the quadrotor formation system.

Motivated on above analyses, to improve control performance, this study focuses on the whole closed-loop stability control algorithm for quadrotor formation modeled with unknown bounded external disturbances and uncertainties. For the characteristics of inner loop and outer loop of quaternion modeled, the different adaptive super twisting control algorithms are designed to improve the convergence rate and accuracy respectively. The finite time stability analysis of whole closed-loop quadrotor formation is proved by a novel Lyapunov function. The main contributions of this paper are summarized as follows:

1) Based on the quaternion model, an super-twisting distributed formation control is designed, which ensures the stability of quadrotor formation under the condition of unknown upper bound of external disturbance. And the stability of closed-loop finite time convergence is proved.

2) For the typical second-order dynamic model, the proposed control law has the advantages of fast convergence speed and high convergence accuracy, which satisfies the speed requirements of quadrotor in fast maneuverability.

The remainder of this paper is organized as follows. In Section II, notations and graph theory, some useful lemmas and problem formulation are given. In Section III, the control laws and adaptive laws are proposed, and the stability of the whole closed-loop system is proven via Lyapunov-based analysis. In Section IV, simulation results are given to demonstrate the effectiveness of the control laws proposed above. Finally, the conclusions are given in Section V.

II. PRELIMINARIES AND PROBLEM STATEMENT

A. GRAPH THEORY

For the formation with n quadrotors, the interaction among the n quadrotors is modelled by weight undirected graph G which is (V, E, F). In undirected graph G, $V = \{v_j, j = 1, \ldots, n\}$ is the set of nodes, $E \subseteq V \times V$ is the set of edges. F is the weighted adjacency matrix of the graph G. For K, we have $a_{ii} = 0$ and, $a_{ji} = 1$ if there is an edge between agent j and agent i while $a_{ji} = 0$ otherwise. The set of neighbors of node v_i is denoted by $(v_j, v_i) \in E$. The out-degree of node v_i is defined as $d_j = \deg_{out}(v_j) = \sum_{j=1}^{n} a_{ji}$. The degree matrix of undirected graph G is $D = diag\{d_1, d_2, \ldots d_n\}$ and the Laplacian matrix of graph G is $K = D - F$. The path from v_j to v_i is a series of different nodes, starting with v_j and ending with v_i, so that the continuous node are adjacent. The physical structure of the quadrotor is shown in Figure 1 [35].

Assumption 1: The communication topology for n agents is connected at the initial time.

B. USEFUL LEMMAS

Lemma 1 [36]: Consider the following nonlinear system $\dot{x}(t) = f(x(t)) + g(x(t))u + \omega$ with $f(0) = 0$. Suppose there exists an open neighborhood Θ of the origin, a C^1 positive-definite function $V{:}\Theta \to \Omega$ and real number $\alpha > 0$, such that $\dot{V} + \alpha V^{\kappa}$ is negative semidefinite on Θ. Then the origin is a finite-time stable equilibrium of nonlinear system.

Lemma 2 [37]: Suppose that there exists a continuous differential positive definite function $V(t)$, and $\alpha > 0, \beta > 0$, $0 < r < 1$ are real numbers. If $V(t)$ satisfies the differential inequality Eq.(1). Then, $V(t)$ will converge to the equilibrium point in a finite time t_f, where t_f can be obtained by Eq.(2)

$$\dot{V} + \alpha V + \beta V^r \leq 0 \tag{1}$$

$$t_f \leq t_0 + \frac{1}{\alpha(1-r)} \ln \frac{\alpha V^{1-r}(x_0) + \beta}{\beta} \tag{2}$$

C. SYSTEM MODEL

Considering that n is the total number of the formation quadrotors, the jth quadrotor is denoted by the subscript j. The

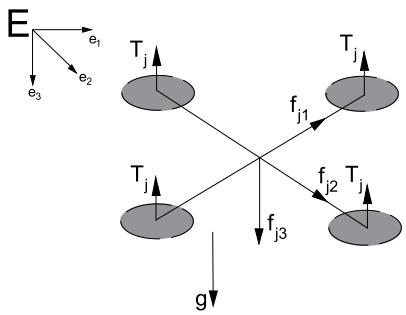

FIGURE 1. Physical structure of a quadrotor.

configuration of quadrotor is shown in Figure 1. To describe the space motion state of the quadrotor, the inertial frame $E = \{e_1, e_2, e_3\}$ with $e_1 = [1, 0, 0]^T$, $e_2 = [0, 1, 0]^T$ and $e_3 = [0, 0, 1]^T$ the unit vectors in the directions x, y, z of the frame E. $F = \{f_{j1}, f_{j2}, f_{j3}\}$ denotes the body-fixed frame of the jth quadrotor, with $f_{j1} = [1, 0, 0]^T$, $f_{j2} = [0, 1, 0]^T$ and $f_{j3} = [0, 0, 1]^T$ the unit vectors in the directions x, y, z of the frame F_j. ω_j is the angular velocity and the orientation is represented by unit-quaternions defined by $Q_j = \left[q_j^T, \eta_j\right]^T$, which is composed of a vector component $q_j = \left[q_{j1}, q_{j2}, q_{j3}\right]^T$ and a scalar component η_j, satisfying

$$q_j^T q_j + \eta_j^2 = 1 \tag{3}$$

The multiplication between two unit-quaternions $Q_1 = [q_1^T, \eta_1]^T$ and $Q_2 = [q_2^T, \eta_2]^T$ are defined by

$$Q_1 \odot Q_2 = \begin{pmatrix} \eta_1 q_2 + \eta_2 q_1 + S(q_1) q_2 \\ \eta_1 \eta_2 - q_2^T q_1 \end{pmatrix} \tag{4}$$

where $\odot$ a non-commutative multiplication operator, $S(\times)$ is the skew-symmetric matrix operator that is defined by

$$S(a) = \begin{bmatrix} 0 & -a_3 & a_2 \\ a_3 & 0 & -a_1 \\ -a_2 & a_1 & 0 \end{bmatrix} \tag{5}$$

where $a = [a_1, a_2, a_3]^T$. Let $R(Q) \in \mathbb{R}^{3\times3}$ denote the Rodriguez rotation matrix from the inertial frame to the body frame, and $R(Q)$ in terms of unit-quaternion can be obtained through the Rodriguez Formula as

$$R(Q) = (\eta^2 - \|q\|^2 I_3 + 2qq^T - 2\eta S(q)) \tag{6}$$

where I_3 is the 3-by-3 identity matrix, $\|\cdot\|$ is the Euclidean norm of vectors.

The model differential equations of the jth quadrotor are expressed as

$$\begin{cases} \dot{p}_j = v_j \\ m_j \dot{v}_j = m_j g e_3 - T_j R(\tilde{Q}_j) e_3 + d_{Uj} \end{cases} \tag{7}$$

$$\begin{cases} \dot{q}_j = \dfrac{1}{2}\left[\eta_j I_3 + S\left(q_j\right)\right]\omega_j \\ \dot{\eta}_j = -\dfrac{1}{2} q_j^T \omega_j \\ I_{fj}\dot{\omega}_j = \Gamma_j - S\left(\omega_j\right) I_{fj}\omega_j + d_{\Gamma j} \end{cases} \tag{8}$$

where m_j is the mass of the jth quadrotor and g is the gravitational acceleration. p_j and v_j are the position and linear velocity expressed in the inertial frame. T_j is the magnitude of the control thrust and $T_j \geq 0$. $\Gamma_j = (\Gamma_{xj}, \Gamma_{yj}, \Gamma_{sj})^T \in \mathbb{R}^3$ represents the control torque applied on the system expressed in the body frame F. d_{Uj} and $d_{\Gamma j}$ are composed of the aerodynamic disturbances and parameter uncertainties. $I_{fj} = diag(I_{xxj}, I_{yyj}, I_{zzj})$ is the symmetric positive definite constant inertia matrix of the jth quadrotor.

Assumption 2: For the formulation control of quadrotors, the communication topology graph is undirected.

Assumption 3: The disturbance d_{Uj} and $d_{\Gamma j}$ are bounded and we denote $\left|d_{Uj}\right| \leq D_{Uj}$ and $\left|d_{\Gamma j}\right| \leq D_{\Gamma j}$, where D_{Uj} and $D_{\Gamma j}$ are unknown upper bound.

D. PROBLEM FORMULATION

Assuming that $p_d = [p_{dx}, p_{dy}, p_{dz}]^T$ and $v_d = [v_{dx}, v_{dy}, v_{dz}]^T$ denote the desired position and velocity of the quadrotor, respectively, and the position and velocity tracking error of the jth quadrotor is defined as

$$\mathrm{e}_{pj} = \sum_{i=0}^{n} a_{ji}(p_j - p_i - \Delta_{ji}) \tag{9}$$

$$\mathrm{e}_{vj} = \sum_{i=0}^{n} a_{ji}(v_j - v_i) \tag{10}$$

where $\Delta_{ji} = [\Delta_{xji}, \Delta_{yji}, \Delta_{zji}]^T$ represents the relative distance between the ith quadrotor and jth quadrotor, which determines the desired formation pattern. For the leader quadrotor, the desired trajectory $\Delta_{ji} = \Delta_{10} = [0, 0, 0]^T$, $p_0 = p_d$, $v_0 = v_d$. Let $Q_d = [q_d^T, \eta_d]^T$ and $q_d = [q_{d1}, q_{d2}, q_{d3}]^T$ denote the desired orientation expressed in the desired frame, and ω_d denotes the desired angular velocity expressed in the desired frame. $\tilde{Q} = [\tilde{q}^T, \tilde{\eta}]^T$ and $\tilde{q} = [\tilde{q}_1, \tilde{q}_2, \tilde{q}_3]^T$ denote the relative orientation error from the body frame to the desired frame, and $\tilde{Q}$ is defined by

$$\tilde{Q} = Q_d^{-1} \odot Q = \begin{pmatrix} \eta_d q - \eta q_d - S(q_d) q \\ \eta_d \eta + q^T q_d \end{pmatrix} \tag{11}$$

where the inverse of the unit-quaternion is defined by $Q^{-1} = [q^T, \eta]^T$. Let ω_d denote the desired angular velocity and the angular velocity error from the body frame to the desired frame $\tilde{\omega}$ is described by

$$\tilde{\omega} = \omega - R\left(\tilde{Q}\right)\omega_d \tag{12}$$

E. CONTROL OBJECTIVES

In this paper, the main objective is to design a formation control law for quadrotor formation to achieve the desired formation pattern and track the desired formation trajectory under parametric uncertainties and external disturbances.

III. FORMATION CONTROL DESIGN

To facilitate the design of formation controller separately, the quadrotor model is divided into the outer-loop subsystem and the inner-loop subsystem. From Eq.(7), it's clear that by designing T_j cannot maintain the stability of jth quadrotor(because it is under-actuated), so, another control input $U_j = T_j R^T(\tilde{Q}_j)e_3$ is designed, which aims to solve under-actuation of the position system. For the system (7) and (8), the outer-loop subsystem and inner-loop subsystem can be written as

Outer-loop subsystem:

$$\begin{cases} \dot{p}_j = v_j \\ m_j \dot{v}_j = m_j g e_3 - U_j + d_{Uj} \end{cases} \tag{13}$$

Inner-loop subsystem:

$$\begin{cases} \dot{q}_j = \dfrac{1}{2}\left[\eta_j I_3 + S\left(q_j\right)\right]\omega_j \\ \dot{\eta}_j = -\dfrac{1}{2} q_j^T \omega_j \\ I_{fj}\dot{\omega}_j = \Gamma_{sj} - S\left(\omega_j\right) I_{fj}\omega_j + d_{\Gamma j} \end{cases} \tag{14}$$

The position formation control for out-loop subsystem and the attitude tracking control for the inner-loop subsystem will be designed respectively.

A. POSITION FORMATION CONTROL DESIGN

The error system can be written in a matrix form as

$$e_{vj} = \dot{e}_{pj} \tag{15}$$

Submitting Eq.(9) to Eq.(15) and it yields

$$\begin{aligned} \dot{e}_{vj} &= \sum_{i=0}^{n} a_{ji}(\dot{v}_j - \dot{v}_i) \\ &= \sum_{i=0}^{n} a_{ji} g e_3 - \sum_{i=0}^{n} a_{ji}\frac{U_j}{m_j} + \sum_{i=0}^{n} a_{ji}\frac{d_{Uj}}{m_j} - \sum_{i=0}^{n} a_{ji}\dot{v}_i \\ &= G_{0j} - \sum_{i=0}^{n} a_{ji}\frac{U_j}{m_j} + \rho_j \end{aligned} \tag{16}$$

where

$$G_{0j} = \sum_{i=0}^{n} a_{ji} g e_3 \tag{17}$$

$$\rho_j = \sum_{i=0}^{n} a_{ji}\frac{d_{U_j}}{m_j} - \sum_{i=0}^{n} a_{ji}\dot{v}_i \tag{18}$$

The virtual displacement controller U_j is designed as following

$$U_j = \frac{m_j}{\sum_{i=0}^{n} a_{ji}}(G_{0j} + b_1(\upsilon(e_{pj}) + 0.5\upsilon(e_{vj}))) \tag{19}$$

where $\upsilon(x) = \begin{cases} \frac{x}{||x||} & x \neq 0 \\ \frac{x}{||x||+\varepsilon_0} & x = 0 \end{cases}$ is the ratio of x to the norm of x, $\varepsilon_0 > 0$ is a very small constant to avoid singularities. $b_1 > 0$ defined as

$$\dot{b}_1 = \begin{cases} -\dfrac{\mu(\frac{4}{\beta_1})^{\frac{3}{4}}}{\frac{2b_1 e_{pj}^T e_{pj} + \|e_{pj}\| e_{vj}^T e_{vj}}{|b_1 - b_1^*|^3} - \frac{4}{\beta_1}} & \|e_{pj}\| \geq \varepsilon_1 \\ 0 & \|e_{pj}\| < \varepsilon_1 \end{cases} \tag{20}$$

Let $U_j = [u_{j1}, u_{j2}, u_{j3}]^T$, so in order to get a unique set of solutions, let $q_{dj3} = 0$, and then we get

$$\begin{bmatrix} u_{j1} \\ u_{j2} \\ u_{j3} \end{bmatrix} = \begin{bmatrix} 2T_j \eta_{dj} q_{dj2} \\ -2T_j \eta_{dj} q_{dj1} \\ T_j[1 - 2(q_{dj1}^2 + q_{dj2}^2)] \end{bmatrix} \tag{21}$$

where

$$u_{j3} = \sqrt{T_j^2 - u_{j1}^2 - u_{j2}^2} \tag{22}$$

So, we can extract the thrust force T_j

$$T_j = \sqrt{u_{j1}^2 + u_{j2}^2 + u_{j3}^2} \tag{23}$$

And the jth η_{dj} exception is

$$\eta_{dj} = \sqrt{\frac{1}{2} + \frac{u_{j3}}{2T_j}} \tag{24}$$

Then, using the first two equations of Eq.(21), extract q_{dj1} and q_{dj2} as

$$q_{dj} = \begin{bmatrix} q_{dj1} \\ q_{dj2} \\ q_{dj3} \end{bmatrix} = \frac{1}{2T_j \eta_{dj}} \begin{bmatrix} -u_{j2} \\ u_{j1} \\ 0 \end{bmatrix} \tag{25}$$

The required angular velocity ω_{dj} can be obtained as

$$\omega_{dj} = 2\begin{bmatrix} \eta_{dj} I_3 + S(q_{dj}) \\ -q_{dj}^T \end{bmatrix}^T \dot{Q}_{dj} \tag{26}$$

Theorem 1: Consider the outer-loop subsystem (7) with the control strategy (19), the tracking error converges to the region around zero within a finite time.

Proof: Choose the following Lyapunov function candidate:

$$\begin{aligned} V &= \|e_{pj}\| s^T A s + \frac{1}{4}(e_{vj}^T e_{vj})^2 + \frac{1}{\beta_1}(b_1 - b_1^*)^4 \\ &= \|e_{pj}\| \begin{bmatrix} \delta(e_{pj}) & e_{vj} \end{bmatrix} \begin{bmatrix} b_1^2 & \frac{\gamma}{2} \\ \frac{\gamma}{2} & b_1 \end{bmatrix} \begin{bmatrix} \delta(e_{pj}) & e_{vj} \end{bmatrix}^T \\ &\quad + \frac{1}{4}(e_{vj}^T e_{vj})^2 + \frac{1}{\beta_1}(b_1 - b_1^*)^4 \\ &= b_1^2 e_{pj}^T e_{pj} + \gamma \|e_{pj}\|^{\frac{1}{2}} e_{pj}^T e_{vj} + b_1 \|e_{pj}\| e_{vj}^T e_{vj} \\ &\quad + \frac{1}{4}(e_{vj}^T e_{vj})^2 + \frac{1}{\beta_1}(b_1 - b_1^*)^4 \end{aligned} \tag{27}$$

where $s = \left[\delta(e_{pj}), e_{vj}^T\right]^T$, let $\gamma < 2b_1^{\frac{3}{2}}, b_1^* > 0, \beta_1 > 0$, $A = \begin{bmatrix} b_1^2 & \frac{\gamma}{2} \\ \frac{\gamma}{2} & b_1 \end{bmatrix}$ is a positive definite symmetric matrix,

$\delta(x) = \begin{cases} \frac{x^T}{\|x\|^{\frac{1}{2}}} & x \neq 0 \\ \frac{x^T}{\|x\|^{\frac{1}{2}}+\varepsilon_0} & x = 0 \end{cases}$ is the ratio of x inverse to the square root of the norm of x.

Consider the Lyapunov function has a number of variables, for the sake of brevity, it is proved in two parts below.

$$V = V_1 + \frac{1}{\beta_1}\left(b_1 - b_1^*\right)^4 \tag{28}$$

where

$$V_1 = V_{11} + V_{12} + V_{13} + V_{14} \tag{29}$$

where

$$V_{11} = b_1^2 e_{pj}^T e_{pj} \tag{30}$$

$$V_{12} = \gamma \left\|e_{pj}\right\|^{\frac{1}{2}} e_{pj}^T e_{vj} \tag{31}$$

$$V_{13} = b_1 \left\|e_{pj}\right\| e_{vj}^T e_{vj} \tag{32}$$

$$V_{14} = \frac{1}{4}(e_{vj}^T e_{vj})^2 \tag{33}$$

The time derivative of Eqs.(29)-(33) are given as follows:

$$\dot{V}_{11} = b_1^2 e_{pj}^T \dot{e}_{pj} \tag{34}$$

$$\dot{V}_{12} = \frac{3}{2}\gamma \left\|e_{pj}\right\|^{\frac{1}{2}} e_{vj}^T e_{vj} + \gamma \left\|e_{pj}\right\|^{\frac{1}{2}} e_{pj}^T \dot{e}_{vj} \tag{35}$$

$$\dot{V}_{13} = b_1 e_{vj}^T e_{vj} \frac{e_{pj}^T}{\left\|e_{pj}\right\|} \dot{e}_{pj} + 2b_1 \left\|e_{pj}\right\| e_{vj}^T \dot{e}_{vj} \tag{36}$$

$$\dot{V}_{14} = e_{vj}^T e_{vj} e_{vj}^T \dot{e}_{vj} \tag{37}$$

Substituting Eq.(16) to Eq.(29), together with Eq.(29)-(33) yields

$$\begin{aligned} \dot{V}_1 &= \dot{V}_{11} + \dot{V}_{12} + \dot{V}_{13} + \dot{V}_{14} \\ &= -\gamma(b_1 + \frac{1}{2}b_1 \upsilon(e_{vj})\theta(e_{pj}) - \theta(e_{pj})\rho_j)\left\|e_{pj}\right\|^{\frac{3}{2}} \\ &\quad - \left\|e_{vj}\right\|(-\frac{3}{2}\gamma \left\|e_{pj}\right\|^{\frac{1}{2}} \left\|e_{vj}\right\| \\ &\quad + (\frac{1}{2}b_1 - \theta(e_{vj})\rho_j)\left\|e_{vj}\right\|^2 \\ &\quad + b_1(b_1 - 2\theta(e_{vj})\rho)\left\|e_{pj}\right\|) \end{aligned} \tag{38}$$

$\theta(x) = \begin{cases} \frac{x^T}{\|x\|} & x \neq 0 \\ \frac{x^T}{\|x\|+\varepsilon_0} & x = 0 \end{cases}$ is the ratio of x inverse to the norm of x.

Assuming that $b_1 > 2C$ and $\left\|\rho_j\right\| \leq C$, then

$$\begin{cases} b_1 + 0.5 \times b_1 \frac{e_{pj}^T e_{vj}}{\left\|e_{pj}\right\|\left\|e_{vj}\right\|} - \frac{e_{pj}^T}{\left\|e_{pj}\right\|}\rho_j \geq 0.5b_1 - C \\ 0.5b_1 - \frac{e_{vj}^T}{\left\|e_{vj}\right\|}\rho \geq 0.5b_1 - C \end{cases} \tag{39}$$

therefore

$$\begin{aligned} \dot{V}_1 &\leq -\gamma(0.5b_1 - C)\left\|e_{pj}\right\|^{\frac{3}{2}} \\ &\quad - \left\|e_{vj}\right\|(-\frac{3}{2}\gamma \left\|e_{pj}\right\|^{\frac{1}{2}} \left\|e_{vj}\right\| + (0.5b_1 - C)\left\|e_{vj}\right\|^2 \\ &\quad + 2b_1 \left\|e_{pj}\right\|(0.5b_1 - C)) \end{aligned} \tag{40}$$

Let

$$\chi = \begin{bmatrix} \left\|e_{pj}\right\|^{\frac{1}{2}} & \left\|e_{vj}\right\| \end{bmatrix}^T$$

$$P = \begin{bmatrix} 2b_1(0.5b_1 - C) & -\frac{3}{4}\gamma \\ -\frac{3}{4}\gamma & 0.5b_1 - C \end{bmatrix}.$$

Submitting it to Eq.(40),then we have

$$\dot{V}_1 \leq -\gamma(0.5b_1 - C)\left\|e_{pj}\right\|^{\frac{3}{2}} - \left\|e_{vj}\right\| \chi^T P \chi \tag{41}$$

Moving forward a single step we can obtain

$$\begin{aligned} \dot{V}_1 &\leq -\gamma \left\|e_{pj}\right\|^{\frac{3}{2}}(0.5b_1 - C) - \left\|e_{vj}\right\|^3 \lambda_{\min}(P) \\ &\leq -M(\left\|e_{pj}\right\|^{\frac{3}{2}} + \left\|e_{vj}\right\|^3) \\ &\leq \frac{-M}{2^{\frac{2}{3}}}(\left\|e_{pj}\right\|^{\frac{1}{2}} + \left\|e_{vj}\right\|)^3 \end{aligned} \tag{42}$$

where

$$\begin{aligned} \chi^T P \chi &\geq \lambda_{\min}(P)(\left\|e_{pj}\right\| + \left\|e_{vj}\right\|^2) \\ &\geq \lambda_{\min}(P)\left\|e_{vj}\right\|^2 \end{aligned} \tag{43}$$

$$(\left\|e_{pj}\right\|^a + \left\|e_{vj}\right\|^a)^{\frac{1}{a}} \leq 2^{\frac{1}{a}-\frac{1}{b}}(\left\|e_{pj}\right\|^b + \left\|e_{vj}\right\|^b)^{\frac{1}{b}}, \quad (a \leq b) \tag{44}$$

$$M = \min\{\gamma(0.5b_1 - C), \lambda_{\min}(P)\} \tag{45}$$

By analyzing the Eq.(43) with Eq.(44), there is

$$\lambda_{\max}(Q)(\left\|e_{pj}\right\|^{\frac{1}{2}} + \left\|e_{vj}\right\|)^4 \geq V_1\left(e_{pj}, e_{vj}\right) \tag{46}$$

so it follows that

$$\lambda_{\max}^{\frac{3}{4}}(Q)(\left\|e_{pj}\right\|^{\frac{1}{2}} + \left\|e_{vj}\right\|)^3 \geq V_1^{\frac{3}{4}}\left(e_{pj}, e_{vj}\right) \tag{47}$$

$$\dot{V}_1 \leq -\frac{M}{2^{\frac{2}{3}}\lambda_{\max}^{\frac{3}{4}}(Q)} V_1^{\frac{3}{4}} \tag{48}$$

From Eq.(28) and Eq.(48), there is

$$\begin{aligned} \dot{V} &= \dot{V}_1 + (2b_1 e_{pj}^T e_{pj} + \left\|e_{pj}\right\| e_{vj}^T e_{vj})\dot{b}_1 \\ &\quad + \frac{4}{\beta_1}(b_1 - b_1^*)^3 \dot{b}_1 \\ &\leq -\frac{M}{2^{\frac{2}{3}}\lambda_{\max}^{\frac{3}{4}}(P)} \dot{V}_1^{\frac{3}{4}}\left(e_{pj}, e_{vj}\right) \\ &\quad + (2b_1 e_{pj}^T e_{pj} + \left\|e_{pj}\right\| e_{vj}^T e_{vj})\dot{b}_1 + \frac{4}{\beta_1}(b_1 - b_1^*)^3 \dot{b}_1 \end{aligned} \tag{49}$$

where $\varepsilon_1$is a constant greater than 0.

Formulation when $\left\|e_{pj}\right\| \geq \varepsilon_1$, $\dot{b}_1 = 0$, getting

$$\dot{V} = \dot{V}_1 \leq -\frac{M}{2^{\frac{2}{3}}\lambda_{\max}^{\frac{3}{4}}(P)} \dot{V}_1^{\frac{3}{4}}\left(e_{pj}, e_{vj}\right) \tag{50}$$

Formulation when $\left\|e_{vj}\right\| < \varepsilon_1$, getting

$$\dot{b}_1 = -\frac{\mu(\frac{4}{\beta_1})^{\frac{3}{4}}}{\frac{2b_1 e_{pj}^T e_{pj} + \left\|e_{pj}\right\| e_{vj}^T e_{vj}}{|b_1 - b_1^*|^3} - \frac{4}{\beta_1}} \tag{51}$$

$$\dot{V} \leq -NV_1^{\frac{3}{4}} + (2b_1 e_{pj}^T e_{pj} + \|e_{pj}\| e_{vj}^T e_{vj})\dot{b}_1 + \frac{4}{\beta_1}(b_1 - b_1^*)^3 \dot{b}_1 - \mu(\frac{4}{\beta_1})^{\frac{3}{4}} |b_1 - b_1^*|^3 + \mu(\frac{4}{\beta_1})^{\frac{3}{4}} |b_1 - b_1^*|^3 \quad (52)$$

where $N = \frac{M}{2^{\frac{2}{3}} \lambda_{\max}^{\frac{3}{4}}(P)}$.

Note that

$$(V_1 + \frac{4}{\beta_1}(b_1 - b_1^*)^4)^{\frac{3}{4}} \leq V_1^{\frac{3}{4}} + \mu(\frac{4}{\beta_1})^{\frac{3}{4}}(b_1 - b_1^*)^3 \quad (53)$$

and

$$-NV_1^{\frac{3}{4}} - \mu(\frac{4}{\beta_1})^{\frac{3}{4}} |b_1 - b_1^*|^3 \leq -\varpi(V_1^{\frac{3}{4}} + (\frac{4}{\beta_1})^{\frac{3}{4}} |b_1 - b_1^*|^3) \quad (54)$$

where $\varpi = \min\{N, \mu\}$

Then we have

$$-\varpi V^{\frac{3}{4}} \geq -\varpi V_1^{\frac{3}{4}} - \mu(\frac{4}{\beta_1})^{\frac{3}{4}} |b_1 - b_1^*|^3 \quad (55)$$

then

$$\dot{V} \leq -\varpi V^{\frac{3}{4}} + (2b_1 e_{pj}^T e_{pj} + \|e_{pj}\| e_{vj}^T e_{vj})\dot{b}_1 + \mu(\frac{4}{\beta_1})^{\frac{3}{4}} |b_1 - b_1^*|^3 \quad (56)$$

It follows that

$$\dot{V} \leq -\varpi V^{\frac{3}{4}} + |b_1 - b_1^*|^3 (\dot{b}_1 (\frac{2b_1 e_{pj}^T e_{pj} + \|e_{pj}\| e_{vj}^T e_{vj}}{|b_1 - b_1^*|^3} - \frac{4}{\beta_1}) + \mu(\frac{4}{\beta_1})^{\frac{3}{4}}) \quad (57)$$

Submitting $\dot{b}_1 = -\frac{\mu(\frac{4}{\beta_1})^{\frac{3}{4}}}{\frac{2b_1 e_{pj}^T e_{pj} + \|e_{pj}\| e_{vj}^T e_{vj}}{|b_1 - b_1^*|^3} - \frac{4}{\beta_1}}$ to Eq.(57), it can be concluded that

$$\dot{V} \leq -\varpi V^{\frac{3}{4}} \quad (58)$$

Thus the outer-loop proof is completed.

Remark 1: The parameter ε_1 affects the convergence rate of position error. In order to accelerate the convergence rate, it should be given a smaller value. The parameter ε_0 is to avoid singularity in the system, it should be as small as possible in its range of values. The parameter b_1 determines the bandwidth of the sliding mode dynamics. A larger b_1 leads to a larger bandwidth indicating a faster response rate and higher tracking accuracy but it will cause larger measurement noises.

B. ATTITUDE CONTROLLER DESIGN

Consider the Inner-loop subsystem (14) and Assumption1-3, let the virtual attitude controller Γ_j be designed as below.

$$\Gamma_j = -I_{fj}\Phi_{1j} - I_{fj}(b_{q1j}\xi_{1j} + s_{1j}) \quad (59)$$

where

$$\Phi_{1j} = \frac{1}{2}(\tilde{\eta}_j I_3 + S(\tilde{q}_j))\tilde{\omega}_j - I_{fj}^{-1} S(\omega_j) I_{fj}\omega_j + S(\tilde{\omega}_j)R(\tilde{Q}_j)\omega_{dj} - R(\tilde{Q}_j)\dot{\omega}_{dj} \quad (60)$$

$$\dot{s}_{1j} = b_{q2j}\xi_{2j} \quad (61)$$

where

$$\xi_{1j} = \frac{e_{qj}}{\|e_{qj}\|^{\frac{1}{2}}} + b_{q3j}|e_{qj}|^r \mathrm{sgn}(e_{qj}) \quad (62)$$

$$\xi_{2j} = \frac{d\xi_{1j}}{de_{qj}}\xi_{1j} = \frac{1}{2}\upsilon(e_{qj}) + \frac{3}{2}b_{q3j}\frac{|e_{qj}|^r}{\|e_{qj}\|^{\frac{1}{2}}}\mathrm{sgn}(e_{qj}) + rb_{q3j}^2|e_{qj}|^{2r-1}\mathrm{sgn}(e_{qj}) \quad (63)$$

$b_{q1j} > 0, b_{q2j} > 0, b_{q3j} > 0$ and

$$\dot{b}_{q1j} = \begin{cases} k\sqrt{\frac{\gamma_1}{2}} & e_{qj} \neq 0 \\ 0 & e_{qj} = 0 \end{cases} \quad (64)$$

$$b_{q2j} = \sigma b_{q1j} \quad (65)$$

where e_{qj} is the error of $\tilde{q}_j$ and $\tilde{\omega}_j$, σ is a constant greater than 0.

$$e_{qj} = \tilde{q}_j + \tilde{\omega}_j \quad (66)$$

Take its first time derivative

$$\begin{aligned}\dot{e}_{qj} &= \dot{\tilde{q}}_j + \dot{\tilde{\omega}}_j \\ &= \frac{1}{2}(\tilde{\eta}_j I_3 + S(\tilde{q}_j))\tilde{\omega}_j + I_{fj}^{-1}\Gamma_j - I_{fj}^{-1}S(\omega_j)I_{fj}\omega_j \\ &\quad + I_{fj}^{-1}d_{\Gamma_j} + S(\tilde{\omega}_j)R(\tilde{Q}_j)\omega_{dj} - R(\tilde{Q}_j)\dot{\omega}_{dj} \\ &= r_j u_j + \Phi_{1j} + \Phi_{2j}\end{aligned} \quad (67)$$

where $r_j = I_{fj}^{-1}$, $u_j = \Gamma_j$, $\Phi_{2j} = I_{fj}^{-1}d_{\Gamma_j}$ and satisfies $\|\dot{\Phi}_{2j}\| \leq L$.

Submitting Eq.(59) and Eq.(61) to the Eq.(67),we can have

$$\dot{e}_{qj} = -b_{q1j}\xi_{1j} + s_{qj} \quad (68)$$

$$\dot{s}_{qj} = -b_{q2j}\xi_2 + \dot{\Phi}_{2j} \quad (69)$$

Theorem 2: Consider the inner-loop subsystem (8) with the control strategy (59), the attitude error converges to the region around zero within a finite time.

Proof: Choose the following Lyapunov function candidate:

$$V_2 = \varsigma_j^T P \varsigma_j + \frac{1}{2\gamma_1}(b_{q1j} - b_{q1j}^*)^2 + \frac{1}{2\gamma_2}(b_{q2j} - b_{q2j}^*)^2 \quad (70)$$

where $\varsigma_j = \begin{bmatrix}\xi_1 & s_{qj}\end{bmatrix}^T$, $P = \begin{bmatrix}\lambda^2 + 4\varepsilon & -\lambda \\ -\lambda & 1\end{bmatrix}$ is a positive definite matrix. and $b_{q1j}^* > 0, b_{q2j}^* > 0, \lambda > 0, \varepsilon > 0$

$$\dot{V}_2 = 2\varsigma_j^T P\dot{\varsigma}_j + \frac{1}{\gamma_1}(b_{q1j} - b_{q1j}^*)\dot{b}_{q1j} + \frac{1}{\gamma_2}(b_{q2j} - b_{q2j}^*)\dot{b}_{q2j} \quad (71)$$

$$\dot{V}_{20} = 2\varsigma_j^T P\dot{\varsigma}_j = -2\frac{d\xi_{1j}}{de_{qj}}\varsigma_j^T Q_1 \varsigma_j \quad (72)$$

where $Q_1 = \begin{bmatrix} Q_{11} & Q_{12} \\ Q_{21} & \lambda \end{bmatrix}$ is a symmetric matrix. in which

$$Q_{11} = b_{q1j}\lambda^2 + 4b_{q1j}\varepsilon - \lambda b_2$$
$$Q_{11} = Q_{21} = \frac{1}{2}(-\lambda^2 - 4\varepsilon - \lambda b_{q1j} + b_2)$$

If $\dot{V}_{20}$ is negative definite, then it needs Q_1 is positive definite, only needing to $\det(Q_1) > 0$. Then it satisfies that

$$-\frac{1}{4}a_1^2 + \frac{1}{2}\lambda b_{q1j}a_1 + \frac{1}{2}b_2 a_1 - \lambda^2 b_2 - \frac{1}{4}\lambda^2 b_{q1j}^2 + \frac{1}{2}\lambda b_{q1j}b_{q2j} - \frac{1}{4}b_2^2 > 0 \quad (73)$$

where

$$a_1 = \lambda^2 + 4\varepsilon \quad (74)$$

So we can get the discriminant $\lambda b_2(b_{q1j} - \lambda) > 0$. Because $\left|\Phi_{2j}\right| \le L$, $\left\|\frac{1}{\xi_{2j}}\right\| \le \vartheta$, we can get $b_{q2j} > \vartheta L$, $b_{q1j} > \lambda$ and $b_2 \in \left[b_{q2j} - \vartheta L, b_{q2j} + \vartheta L\right]$

Let $\det(Q_1) = 0$, we can get

$$b_{1j}^+ = \lambda b_{q1j} + b_2 + 2\sqrt{\lambda b_2(b_{q1j} - \lambda)}$$
$$b_{1j}^- = \lambda b_{q1j} + b_2 - 2\sqrt{\lambda b_2(b_{q1j} - \lambda)} \quad (75)$$

It's obvious that $b_{1j}^+ > b_{1j}^-$, if $a_1 \in \left[b_{1j}^-, b_{1j}^+\right]$, then we can get that the matrix Q_1 is positive defined.

Taking into account a well-known inequality $\lambda_{\min}(Q_1)\|\varsigma_j\|^2 \le \varsigma_j^T Q \varsigma_j$ with Eq.(72), there is

$$\begin{aligned}
\dot{V}_{20} &\le -\frac{d\xi_{1j}}{de_{qj}}\|\varsigma\|^2\lambda_{\min}\{Q_1\} \\
&\le -\frac{d\xi_{1j}}{de_{qj}}\frac{V_{20}\lambda_{\min}\{Q_1\}}{\lambda_{\max}\{P_1\}} \\
&\le -\left(\frac{\kappa}{2\|e_{qj}\|} + \kappa b_{q3j}\right)\frac{V_{20}\lambda_{\min}\{Q_1\}}{\lambda_{\max}\{Q_1\}} \\
&\le -\frac{\kappa}{2\|\varsigma\|}\frac{V_{20}\lambda_{\min}\{Q_1\}}{\lambda_{\max}\{Q_1\}} - \kappa b_{q3j}\frac{V_{20}\lambda_{\min}\{Q_1\}}{\lambda_{\max}\{Q_1\}} \\
&\le -\frac{\kappa\lambda_{\min}\{Q_1\}\lambda_{\min}^{\frac{1}{2}}\{Q_1\}}{\lambda_{\max}\{Q_1\}}V_{20}^{\frac{1}{2}} - \frac{\kappa b_{q3j}\lambda_{\min}\{Q_1\}}{\lambda_{\max}\{Q_1\}}V_{20} \\
&\le -N_1 V_{20}^{\frac{1}{2}}
\end{aligned} \quad (76)$$

where $N_1 = \frac{\kappa\lambda_{\min}\{Q_1\}\lambda_{\min}^{\frac{1}{2}}\{P_1\}}{\lambda_{\max}\{P_1\}}$, κ is a constant and $\kappa \le \frac{1+rb_{q3j}|w|^{r-1}}{1+b_{q3j}}$

Substituting (76) to (71), there is

$$\begin{aligned}
\dot{V}_2 &= \dot{V}_{20} + \frac{1}{\gamma_1}(b_{q1j} - b_{q1j}^*)\dot{b}_{q1j} + \frac{1}{\gamma_2}(b_{q2j} - b_{q2j}^*)\dot{b}_{q2j} \\
&\le -N_1 V_{20}^{\frac{1}{2}} + \frac{1}{\gamma_1}(b_{q1j} - b_{q1j}^*)\dot{b}_{q1j} + \frac{1}{\gamma_2}(b_{q2j} - b_{q2j}^*)\dot{b}_{q2j} \\
&= -N_1 V_{20}^{\frac{1}{2}} - \frac{N_2}{\sqrt{2\gamma_1}}\left|b_{q1j} - b_{q1j}^*\right| - \frac{N_3}{\sqrt{2\gamma_2}}\left|b_{q2j} - b_{q2j}^*\right| \\
&\quad + \frac{1}{\gamma_1}(b_{q1j} - b_{q1j}^*)\dot{b}_{q1j} + \frac{1}{\gamma_2}(b_{q2j} - b_{q2j}^*)\dot{b}_{q2j} \\
&\quad + \frac{N_2}{\sqrt{2\gamma_1}}\left|b_{q1j} - b_{q1j}^*\right| + \frac{N_3}{\sqrt{2\gamma_2}}\left|b_{q2j} - b_{q2j}^*\right| \\
&\le -\varpi_2 V_2^{\frac{1}{2}} + \frac{1}{\gamma_1}(b_{q1j} - b_{q1j}^*)\dot{b}_{q1j} + \frac{1}{\gamma_2}(b_{q2j} - b_{q2j}^*)\dot{b}_{q2j} \\
&\quad + \frac{N_2}{\sqrt{2\gamma_1}}\left|b_{q1j} - b_{q1j}^*\right| + \frac{N_3}{\sqrt{2\gamma_2}}\left|b_{q2j} - b_{q2j}^*\right|
\end{aligned} \quad (77)$$

where b_{q1j}, b_{q2j} are both bounded, by selecting b_{q1j}^*, b_{q2j}^* there is $b_{q1j} - b_{q1j}^* < 0$, $b_{q2j} - b_{q2j}^* < 0$. $N_2 > 0$ and $N_3 > 0$ are both constants, $\varpi_2 = \min\{N_1, N_2, N_3\}$

The Eq.(77) can be rewritten as

$$\begin{aligned}
\dot{V}_2 &\le -\varpi_2 V_2^{\frac{1}{2}} - \left|b_{q1j} - b_{q1j}^*\right|\left(\frac{1}{\gamma_1}\dot{b}_{q1j} - \frac{N_2}{\sqrt{2\gamma_1}}\right) \\
&\quad - \left|b_{q2j} - b_{q2j}^*\right|\left(\frac{1}{\gamma_2}\dot{b}_{q2j} - \frac{N_3}{\sqrt{2\gamma_2}}\right) \\
&= -\varpi_2 V_2^{\frac{1}{2}} + \tau
\end{aligned} \quad (78)$$

where

$$\tau = -\left|b_{q1j} - b_{q1j}^*\right|\left(\frac{1}{\gamma_1}\dot{b}_{q1j} - \frac{N_2}{\sqrt{2\gamma_1}}\right) - \left|b_{q2j} - b_{q2j}^*\right|\left(\frac{1}{\gamma_2}\dot{b}_{q2j} - \frac{N_3}{\sqrt{2\gamma_2}}\right) \quad (79)$$

If $e_{qj} \ne 0$, there is $\dot{b}_{q1j} = k\sqrt{\frac{\gamma_1}{2}}$ and

$$\tau = -\left|b_{q2j} - b_{q2j}^*\right|\left(\frac{1}{\gamma_2}\dot{b}_{q2j} - \frac{N_3}{\sqrt{2\gamma_2}}\right) \quad (80)$$

By selecting $\sigma = \frac{N_3}{2N_2}\sqrt{\frac{\gamma_2}{\gamma_1}}$, we can get that

$$\begin{aligned}
\dot{b}_{q2j} &= 2\sigma\dot{b}_{q1j} \to \dot{b}_{q2j} \\
&= \sigma N_2\sqrt{2\gamma_1} \to \dot{b}_{q2j} = N_2\sqrt{\frac{\gamma_2}{2}}
\end{aligned} \quad (81)$$

So there is $\tau = 0$, substitute it to (78), then there is

$$\dot{V}_2 \le -\varpi_2 V_2^{\frac{1}{2}} \quad (82)$$

Thus the inner-loop proof is completed.

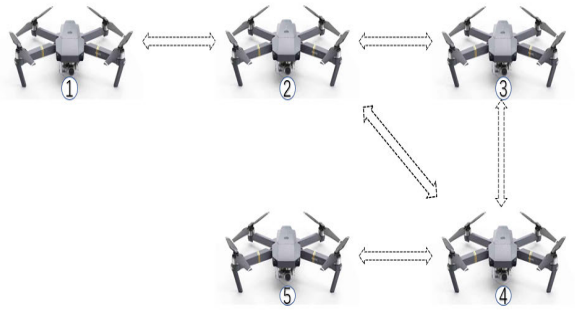

FIGURE 2. The communication graph.

TABLE 1. Initial values of the control.

State	Position(m)	Velocity(m/s)	Quarternion	Expected quarternion	Angular velocity(rad)	Expected angular velocity
quadrotor1	[1;2;2]	[0;0;0]	[0;0;0.6;0.8]	[0;0;0;0]	[0;0;0]	[0;0;0]
quadrotor2	[2;1;3]	[0;0;0]	[0;0;0.6;0.8]	[0;0;0;0]	[0;0;0]	[0;0;0]
quadrotor3	[3;2;3]	[0;0;0]	[0;0;0.6;0.8]	[0;0;0;0]	[0;0;0]	[0;0;0]
quadrotor4	[2;-1;2]	[0;0;0]	[0;0;0.6;0.8]	[0;0;0;0]	[0;0;0]	[0;0;0]
quadrotor5	[1;1;2]	[0;0;0]	[0;0;0.6;0.8]	[0;0;0;0]	[0;0;0]	[0;0;0]

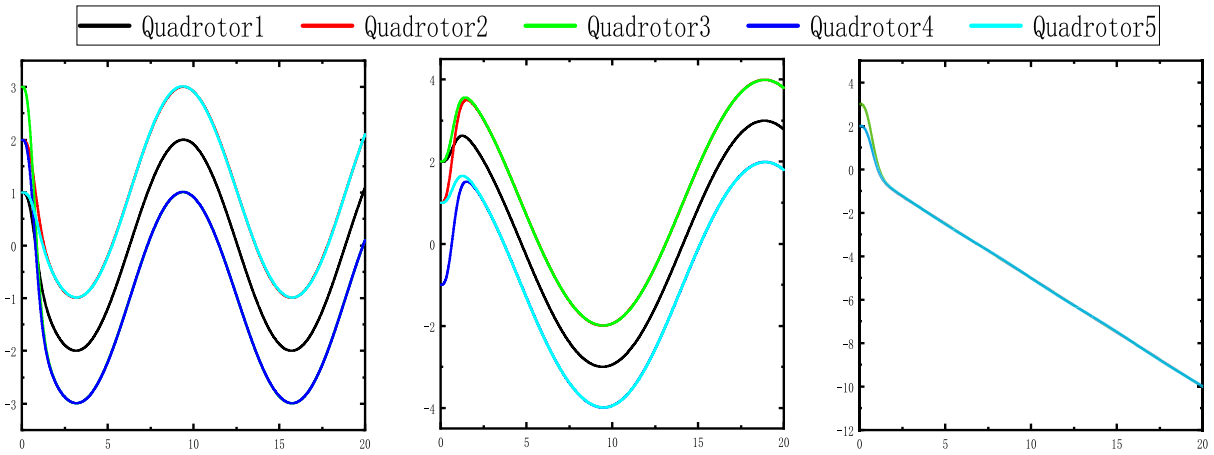

FIGURE 3. Formation tracking trajectory of five quadrotors.

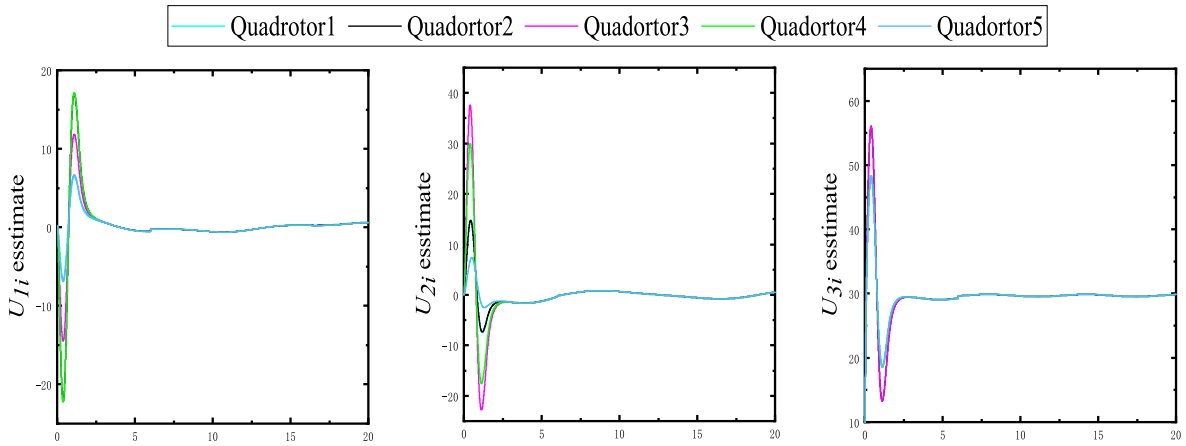

FIGURE 4. Control forces of the ASTDFC.

Remark 2: The parameter k in Eq.(64) will affect the convergence of attitude error of quadrotor. A larger k leads to faster convergence but at the cost of introducing more measurement noises. The parameter λ also affects the convergence of attitude error of quadrotor and it is suggested to be in the range of $1 < \lambda < 3$.

C. CONVERGENCE ANALYSIS OF THE CLOSE-LOOP SYSTEM

In section III.A and III.B, the stability analysis of the outer-loop and inner-loop have been proved. In this section, we will prove the stability analysis and convergence characteristic for the closed-loop of quadrotor formation.

Theorem 3: For the whole closed-loop system given by outer-loop subsystem (13) controller by (19) with adaptive law (20) and inner-loop subsystem (14) controller by (59) with adaptive law (64) under the upper bounded disturbances and uncertainties. The whole closed-loop system is input-state stable in finite convergence time. To this end, the control objectives can be established.

Proof: Consider the Lyapunov function candidate of whole closed-loop system as follows:

$$V_{whole} = V_{outer} + V_{inner} \tag{83}$$

where V_{outer} and V_{inner} are the Lyapunov function of outer-loop system and inner-loop system. As V_{outer} and V_{inner} are positive definite, the whole closed-loop system Lyapunov

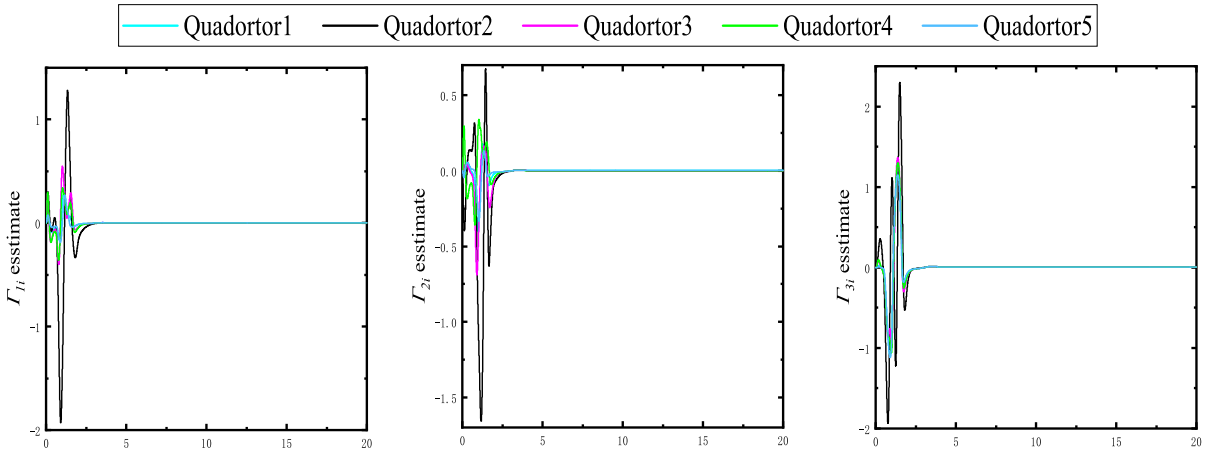

FIGURE 5. Control torques of the ASTDFC.

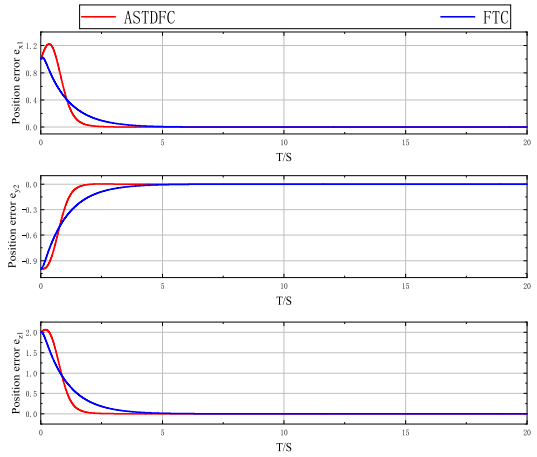

FIGURE 6. ASTDFC and FTC comparison of position errors for quadrotor 1.

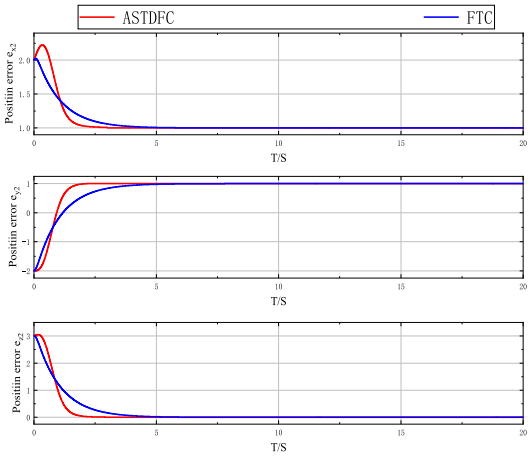

FIGURE 7. ASTDFC and FTC comparison of position errors for quadrotor 2.

function is positive definite. Differentiating the Lyapunov function V_{whole} along the trajectory of the system, we can derive that

$$\begin{aligned}\dot{V}_{whole} &= \dot{V}_{outer} + \dot{V}_{inner} \\ &\leq -\min\{N, \mu\} V_{outer}^{\frac{3}{4}} - \min\{N_1, N_2, N_3\} V_{inner}^{\frac{1}{2}}\end{aligned} \tag{84}$$

For the convenience of the proof, divide the space $[V_{outer}, V_{inner}]^T \in \Re^{+2}$ into two different areas, O and R, area R further divided into two areas R_1 and R_2, which are defined as follows:

$$O = \{(V_{outer}, V_{inner}) : V_{outer} \geq 1\} \tag{85}$$

$$R = R_1 \cup R_2 \tag{86}$$

$$R_1 = \{(V_{outer}, V_{inner}) : V_{outer} < 1 \& V_{inner} < 1\} \tag{87}$$

$$R_2 = \{(V_{outer}, V_{inner}) : V_{outer} < 1 \& V_{inner} \geq 1\} \tag{88}$$

When $[V_{outer}, V_{inner}]$ is in the area O, Eq.(84) can be rewritten as:

$$\begin{aligned}\dot{V}_{whole} &\leq -\min\{\min\{N, \mu\}, \min\{N_1, N_2, N_3\}\} \\ &\quad \left(V_{outer}^{\frac{1}{2}} + V_{inner}^{\frac{1}{2}}\right) \\ &\leq -\min\{\min\{N, \mu\}, \min\{N_1, N_2, N_3\}\} V_{whole}^{\frac{1}{2}}\end{aligned} \tag{89}$$

When $[V_{outer}, V_{inner}]$ is in the area R. First, in the area R_1, Eq.(89) can be rewritten as:

$$\begin{aligned}\dot{V}_{whole} &\leq -\min\{\min\{N, \mu\}, \min\{N_1, N_2, N_3\}\} \\ &\quad \left(V_{outer}^{\frac{3}{4}} + V_{inner}^{\frac{3}{4}}\right) \\ &\leq -\min\{\min\{N, \mu\}, \min\{N_1, N_2, N_3\}\} V_{whole}^{\frac{3}{4}}\end{aligned} \tag{90}$$

From Theorem 1, the space can be satisfied to be stable in finite time as shown in Eq.(89) and Eq.(90). And it is hard to determine the convergence characteristic in the area, because the outer-loop and inner-loop Lyapunov function cannot be easily replaced to satisfy the finite time convergence theorem. However, it does not affect the proof.

As shown in theorem 2, the independent inner-loop system can be stable within finite time. The inner-loop Lyapunov

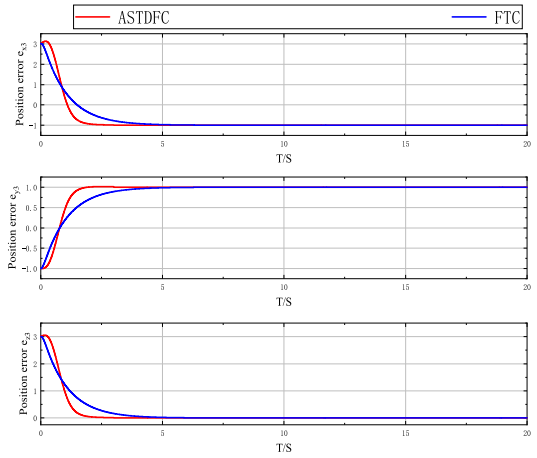

FIGURE 8. ASTDFC and FTC comparison of position errors for quadrotor 3.

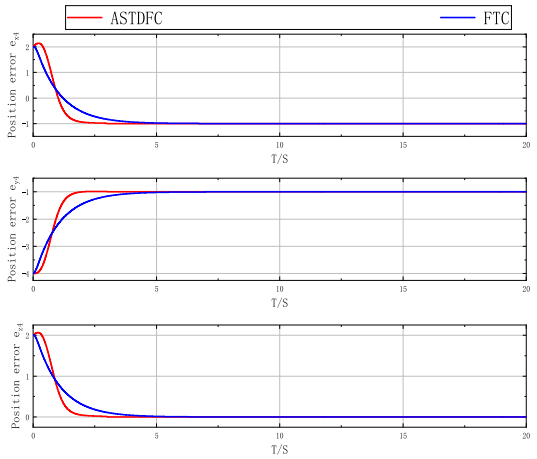

FIGURE 9. ASTDFC and FTC comparison of position errors for quadrotor 4.

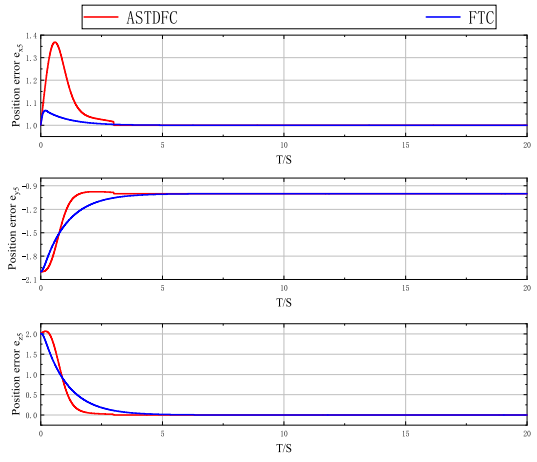

FIGURE 10. ASTDFC and FTC comparison of position errors for quadrotor 5.

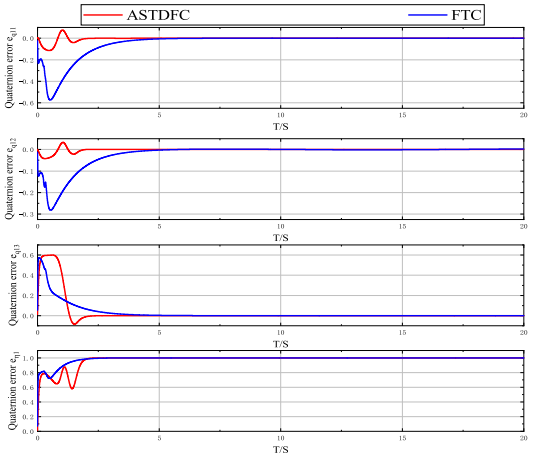

FIGURE 11. Quaternion tracking errors of quadrotor 1.

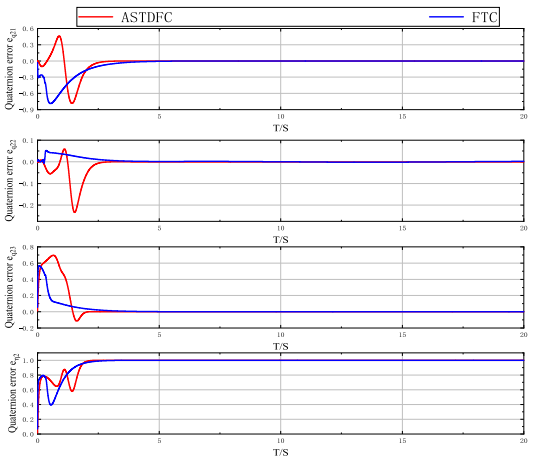

FIGURE 12. Quaternion tracking errors of quadrotor2.

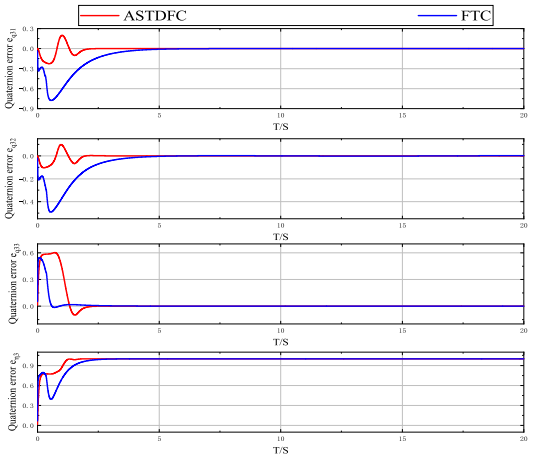

FIGURE 13. Quaternion tracking errors of quadrotor 3.

function also will convergence to zero. Hence, the space $[V_{outer}, V_{inner}]^T \in \Re^{+2}$ will not stay in R_2 forever, but cross from R_2 to R_1 within the finite time. Once the space enter R_1. Therefore, the finite time stability of whole closed-loop system can be guaranteed.

Thus the proofs are completed.

IV. SIMULATION

To prove the effectiveness of the proposed control laws and adaptive laws for the formation modeled on quaternion, several simulations are carried out in this section. In this section, we suppose a quadrotor formation including five quadrotors. Quadrotor communicates with other quadrotor within the

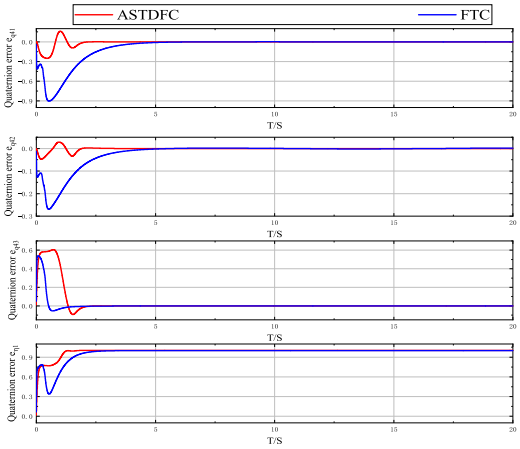

FIGURE 14. Quaternion tracking errors of quadrotor 4.

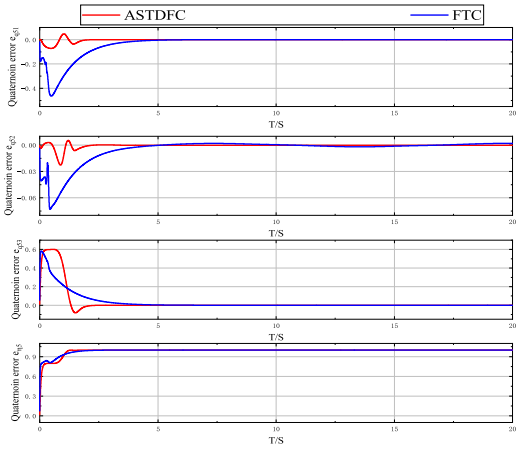

FIGURE 15. Quaternion tracking errors of quadrotor 5.

TABLE 2. The parameters setting of the five quadrotors.

parameters	value	parameters	value
μ	12	σ	2
β	2	g	$9.8m/s^2$
b_{q3j}	1	γ_1	2
k	10	I_{fj}	$diag(0.039, 0.039, 0.12)kg \cdot m^2$
ε_1	0.22(deg)	ε_0	0.01

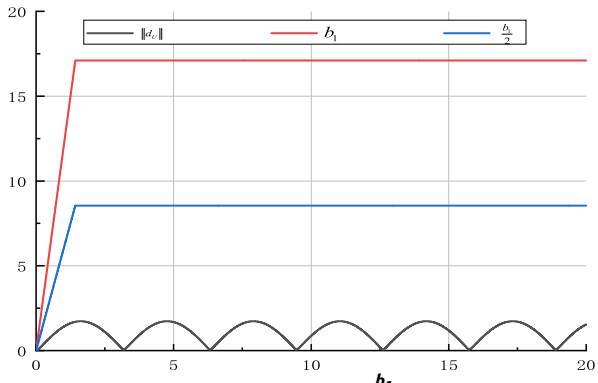

FIGURE 16. Curves of adaptive gains b_1 and $\frac{b_1}{2}$.

range of communication, and the communication graph is presented in Figure 2. Five quadrotors have different initial

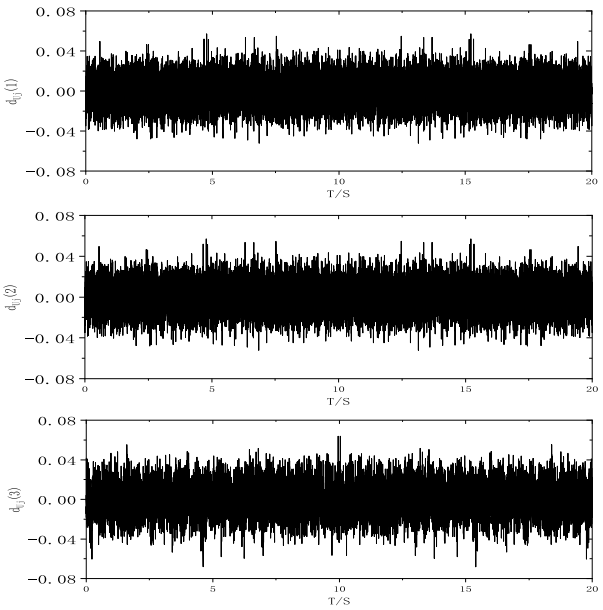

FIGURE 17. Real white Gaussian noises of power on position subsystem.

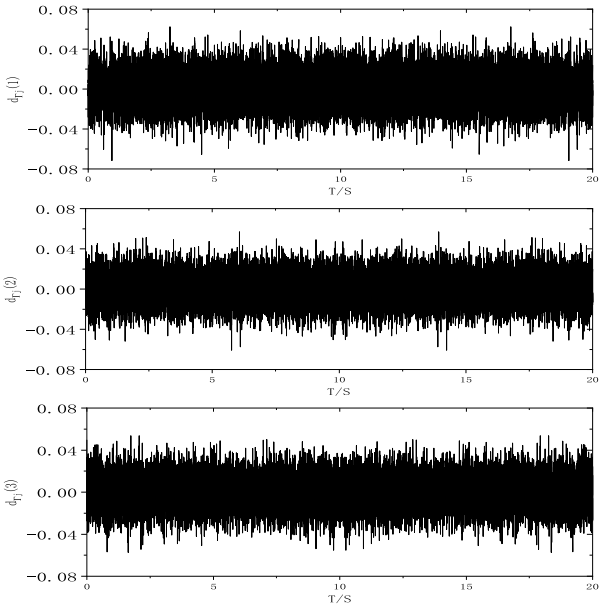

FIGURE 18. Real white Gaussian noises of power on attitude subsystem.

position and attitude. The simulation will verify that quadrotors can form and maintain the formation with high performance by using the proposed control method. For further prove the superiority of proposed algorithm, it is compared with the finite time convergence control algorithm in [20] with quaternion-based system.

A. SIMULATION I

B. PARAMETERS SETTING

Assuming that the leader quadrotor flies along the predetermined trajectory: the reference trajectory of the leader used

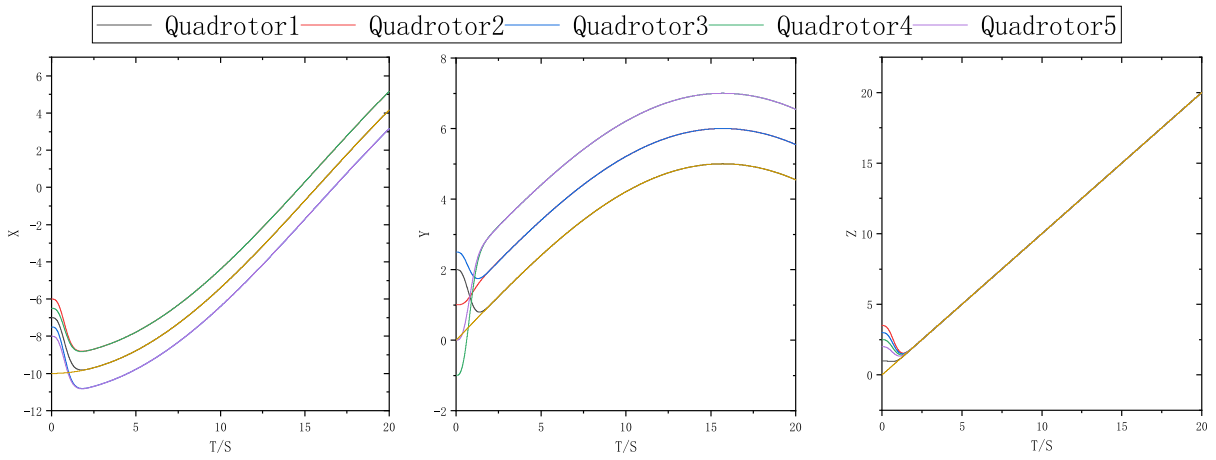

FIGURE 19. Position tracking on x, y, and z axis.

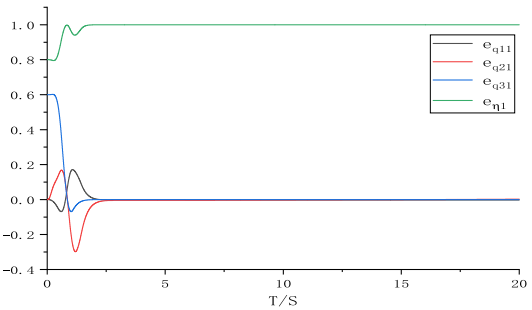

FIGURE 20. Quaternion tracking errors of quadrotor 1.

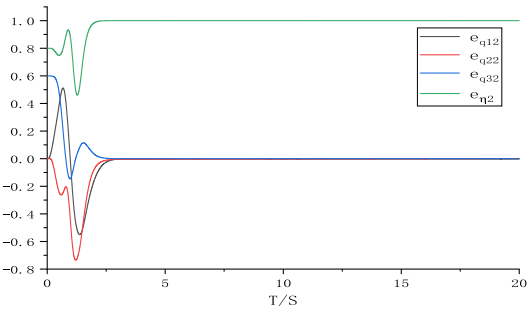

FIGURE 21. Quaternion tracking errors of quadrotor 2.

in the simulation can be expressed as:

$$P_d = \left[-2\sin\frac{t}{2}, 3\cos\frac{t}{3}, -\frac{t}{2}\right]^T$$

To verify the validity of the adaptive law equation (19) and (59), the disturbances of outer-loop and the inner-loop are given by $d_{Uj} = [\sin t, \sin t, \sin t]^T$, $d_{\Gamma j} = [\sin \pi t, \sin \pi t, \sin \pi t]^T$, for j = 1, 2, 3, 4, 5. The initial values and desired trajectory of each quadrotor are given in Table 1, and the parameters of the controllers and proof process are shown in Table 2.

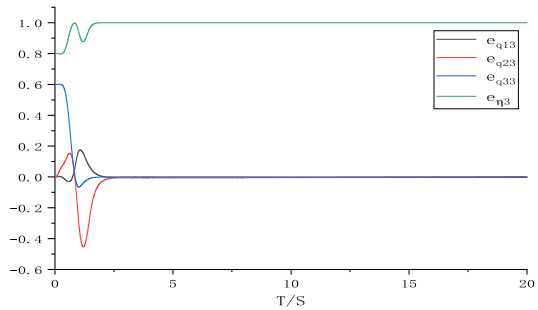

FIGURE 22. Quaternion tracking errors of quadrotor 3.

C. SIMULATION RESULTS

In this part, we compare the proposed algorithm with finite time control(FTC) algorithm [20], and the purpose of this comparison is to explain which method can form and maintain the formation configuration with higher precision and faster convergence speed.

The simulation results are provided in Figure 3-Figure 16. Figure 3 shows the x-coordination, y-coordination and z-coordination trajectories of five quadrotors with proposed algorithm. Figure 4 and Figure 5 show the control forces and torques of the ASTDFC. And Figures 6-15 show the comparison results between the two algorithms. From Figure 16, the curve changes of the adaptive law and disturbance are clearly presented.

Figure 3 shows the control strategy designed in this paper can form and maintain formation quickly in the x y z plane. From Figure 4 and Figure 5, it can be observed that the control forces and torques can converge in short time. Figures 6-9 illustrate that the method proposed in this paper converge to 0 within 2s, which is faster than that by finite time convergence method. Moreover, the errors convergences to 0 with higher convergence precision and faster convergence rate by the proposed algorithm. From Figures 10-15, it can be observed that convergence of ASTDFC is faster than FTC.

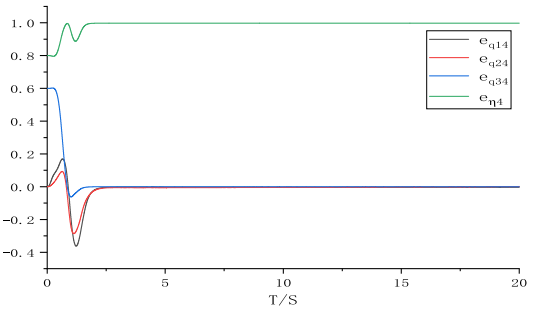

FIGURE 23. Quaternion tracking errors of quadrotor 4.

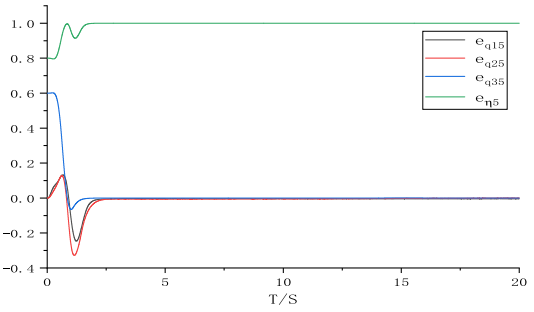

FIGURE 24. Quaternion tracking errors of quadrotor 5.

In Figure 16, it's clear that both the adaptive b_1 and $\frac{b_1}{2}$ are larger than the disturbance $\|d_{Uj}\|$, and finite-time stability can be established.

D. SIMULATION II

In this section, we test the convergence performance of quadrotor formation under irregular disturbances. The Real white Gaussian noises are considered as the irregular disturbances. We design a new trajectory for the quadrotor formation, and the other parameters are the same as in Simulation I. The reference linear velocity is

$$v_d = \begin{bmatrix} \sin(0.1t) & 0.5\cos(0.1t) & 1 \end{bmatrix}$$

The simulation results are shown in Figure 17 - Figure 24. Figures 17-18 show the noise added to the position subsystem and attitude subsystem. Figure 19 is the specific trajectory of the quadrotor formation in three directions. Figures 20-24 show the quaternion errors of each quadrotor.

As shown in Figure 19, it can be seen that the quadrotor formation can maintain unity at about 2.5s. From Figures 20-24, it can be seen that the quaternion errors of each quadrotor can converge before 3s. From these figures, it can be seen that the proposed method has an improved tracking performance of the closed-loop control system.

V. CONCLUSION

Distributed formation control problem for multi-quadrotors described by unit-quaternions has been studied in this paper. Based on super-twisting control and finite time control method, considering the characteristic of the position subsystem and attitude subsystem, the different control methods are developed and adopted to improve the convergence rate and accuracy of the system respectively. Then with the theoretical analysis, the stability of whole closed-loop system is proved and quadrotor formation can converge to the desired formation configures in finite time. Finally, the effectiveness of the proposed method has been illustrated with numerous simulations. In the future work, the actuator deadzones, unmodeled dynamics and other practical problems will considered. The hardware implementation of quadrotor formation will be developed, and the simulation results will be compared with the actual results.

REFERENCES

[1] R. Ramsankaran, P. J. Navinkumar, A. Dashora, and A. V. Kulkarni, "UAV-based survey of glaciers in himalayas: Challenges and recommendations," *J. Indian Soc. Remote Sens.*, vol. 49, no. 5, pp. 1171–1187, May 2021.

[2] K. Boudjit and N. Ramzan, "Human detection based on deep learning YOLO-v2 for real-time UAV applications," *J. Exp. Theor. Artif. Intell.*, vol. 9, pp. 1–18, Apr. 2021.

[3] X. Jiang, X. Chen, J. Tang, N. Zhao, X. Y. Zhang, D. Niyato, and K.-K. Wong, "Covert communication in UAV-assisted air-ground networks," *IEEE Wireless Commun.*, vol. 28, no. 4, pp. 190–197, Aug. 2021.

[4] J. Haskins, C. Endris, A. S. Thomsen, F. Gerbl, M. C. Fountain, and K. Wasson, "UAV to inform restoration: A case study from a California tidal Marsh," *Frontiers Environ. Sci.*, vol. 9, Apr. 2021, Art. no. 642906.

[5] N. Delavarpour, C. Koparan, J. Nowatzki, S. Bajwa, and X. Sun, "A technical study on UAV characteristics for precision agriculture applications and associated practical challenges," *Remote Sens.*, vol. 13, no. 6, p. 1204, Mar. 2021.

[6] B. Mu, H. Li, J. Ding, and Y. Shi, "Consensus in second-order multiple flying vehicles with random delays governed by a Markov chain," *J. Franklin Inst.*, vol. 352, no. 9, pp. 3628–3644, Sep. 2015.

[7] B. Mu, K. Zhang, and Y. Shi, "Integral sliding mode flight controller design for a quadrotor and the application in a heterogeneous multi-agent system," *IEEE Trans. Ind. Electron.*, vol. 64, no. 12, pp. 9389–9398, Dec. 2017.

[8] T. Kopfstedt, M. Mukai, M. Fujita, and C. Ament, "Control of formations of UAVs for surveillance and reconnaissance missions," *IFAC Proc. Volumes*, vol. 41, no. 2, pp. 5161–5166, 2008.

[9] S. Minaeian, J. Liu, and Y. J. Son, "Vision-based target detection and localization via a team of cooperative UAV and UGVs," *IEEE Trans. Syst., Man, Cybern., Syst.*, vol. 46, no. 7, pp. 1005–1016, Jul. 2017.

[10] X. Z. Jin, S. F. Wang, G. H. Yang, and D. Ye, "Robust adaptive hierarchical insensitive tracking control of a class of leader-follower agents," *Inf. Sci.*, vol. 406, pp. 234–247, Sep. 2017.

[11] G. Sun, R. Zhou, K. Xu, Z. Weng, Y. Zhang, Z. Dong, and Y. Wang, "Cooperative formation control of multiple aerial vehicles based on guidance route in a complex task environment," *Chin. J. Aeronaut.*, vol. 33, no. 2, pp. 701–720, Feb. 2020.

[12] W. Zhongsheng, Y. Sen, and D. Hairui, "Quadrotor formation inversion control method based on unit quaternion," *Int. J. Adv. Netw., Monitor. Controls*, vol. 3, no. 1, pp. 27–34, 2018.

[13] W. Zhao and T. H. Go, "Quadcopter formation flight control combining MPC and robust feedback linearization," *J. Franklin Inst.*, vol. 351, no. 3, pp. 1335–1355, 2014.

[14] N. Xuan-Mung and S. K. Hong, "Robust adaptive formation control of quadcopters based on a leader–follower approach," *Int. J. Adv. Robotic Syst.*, vol. 16, no. 4, Jul. 2019, Art. no. 172988141986273.

[15] D. Galzi and Y. Shtessel, "UAV formations control using high order sliding modes," in *Proc. Amer. Control Conf.*, vol. 30, Jun. 2006, p. 6.

[16] M. Turpin, N. Michael, and V. Kumar, "Trajectory design and control for aggressive formation flight with quadrotors," *Auto. Robots*, vol. 33, nos. 1–2, pp. 143–156, Aug. 2012.

[17] Y. Chen and Y. Shi, "Consensus for linear multiagent systems with time-varying delays: A frequency domain perspective," *IEEE Trans. Cybern.*, vol. 47, no. 8, pp. 2143–2150, Aug. 2017, doi: 10.1109/TCYB.2016.2590480.

[18] X. Ai and J. Yu, "Flatness-based finite-time leader–follower formation control of multiple quadrotors with external disturbances," *Aerosp. Sci. Technol.*, vol. 92, pp. 20–33, Sep. 2019.

[19] W. Jasim and D. Gu, "Robust team formation control for quadrotors," *IEEE Trans. Control Syst. Technol.*, vol. 26, no. 4, pp. 1516–1523, Jul. 2018.

[20] H. Liu, T. Ma, F. L. Lewis, and Y. Wan, "Robust formation control for multiple quadrotors with nonlinearities and disturbances," *IEEE Trans. Cybern.*, vol. 50, no. 4, pp. 1362–1371, Apr. 2020.

[21] H. Du, W. Zhu, G. Wen, Z. Duan, and J. Lu, "Distributed formation control of multiple quadrotor aircraft based on nonsmooth consensus algorithms," *IEEE Trans. Cybern.*, vol. 49, no. 1, pp. 342–353, Jan. 2019.

[22] H. Du, W. Zhu, G. Wen, and D. Wu, "Finite-time formation control for a group of quadrotor aircraft," *Aerosp. Sci. Technol.*, vol. 69, pp. 609–616, Oct. 2017.

[23] J. Wang and M. Xin, "Integrated optimal formation control of multiple unmanned aerial vehicles," *IEEE Trans. Control Syst. Technol.*, vol. 21, no. 5, pp. 1731–1744, Sep. 2013.

[24] J. Wang, L. Han, X. Dong, Q. Li, and Z. Ren, "Distributed sliding mode control for time-varying formation tracking of multi-UAV system with a dynamic leader," *Aerosp. Sci. Technol.*, vol. 111, Apr. 2021, Art. no. 106549.

[25] F. Chen, R. Jiang, K. Zhang, B. Jiang, and G. Tao, "Robust backstepping sliding-mode control and observer-based fault estimation for a quadrotor UAV," *IEEE Trans. Ind. Electron.*, vol. 63, no. 8, pp. 5044–5056, Aug. 2016.

[26] A. K. Khotimah, E. Apriliani, and M. Lijah, "Control strategy of unmanned aerial vehicle (UAV) by using sliding mode control method," *Int. J. Eng. Trends Technol.*, vol. 2020, pp. 82–86, Oct. 2020.

[27] N. Sun, T. Yang, Y. Fang, Y. Wu, and H. Chen, "Transportation control of double-pendulum cranes with a nonlinear quasi-PID scheme: Design and experiments," *IEEE Trans. Syst., Man, Cybern., Syst.*, vol. 49, no. 7, pp. 1408–1418, Jul. 2019, doi: 10.1109/TSMC.2018.2871627.

[28] T. Yang, N. Sun, and Y. Fang, "Adaptive fuzzy control for a class of MIMO underactuated systems with plant uncertainties and actuator deadzones: Design and experiments," *IEEE Trans. Cybern.*, early access, Feb. 2, 2021, doi: 10.1109/TCYB.2021.3050475.

[29] L. Zhao, C. Zheng, Y. Wang, and B. Liu, "A finite-time control for a pneumatic cylinder servo system based on a super-twisting extended state observer," *IEEE Trans. Syst., Man, Cybern., Syst.*, vol. 51, no. 2, pp. 1164–1173, Feb. 2021, doi: 10.1109/TSMC.2019.2895873.

[30] L. Guo, D. Wang, Z. Peng, and L. Diao, "Improved super-twisting sliding mode control of a stand-alone DFIG-DC system with harmonic current suppression," *IET Power Electron.*, vol. 13, no. 7, pp. 1311–1320, May 2020.

[31] H. Komurcugil and S. Bayhan, "Super-twisting sliding mode control for grid-tied T-type qZSI with reduced capacitor voltage," in *Proc. IEEE 29th Int. Symp. Ind. Electron. (ISIE)*, Jun. 2020, pp. 790–795.

[32] J. Liu, M. Sun, Z. Chen, and Q. Sun, "Super-twisting sliding mode control for aircraft at high angle of attack based on finite-time extended state observer," *Nonlinear Dyn.*, vol. 99, no. 4, pp. 2785–2799, Mar. 2020, doi: 10.1007/s11071-020-05481-1.

[33] F. Zhang and P. Huang, "Fuzzy-based adaptive super-twisting sliding-mode control for a maneuverable tethered space net robot," *IEEE Trans. Fuzzy Syst.*, vol. 29, no. 7, pp. 1739–1749, Jul. 2021.

[34] S. Ahmed, A. Ahmed, I. Mansoor, F. Junejo, and A. Saeed, "Output feedback adaptive fractional-order super-twisting sliding mode control of robotic manipulator," *Iranian J. Sci. Technol., Trans. Electr. Eng.*, vol. 45, no. 1, pp. 335–347, Mar. 2021.

[35] W. Shang, G. Jing, D. Zhang, T. Chen, and Q. Liang, "Adaptive fixed time nonsingular terminal sliding-mode control for quadrotor formation with obstacle and inter-quadrotor avoidance," *IEEE Access*, vol. 9, pp. 60640–60657, 2021, doi: 10.1109/ACCESS.2021.3074316.

[36] S. P. Bhat and D. S. Bernstein, "Finite-time stability of homogeneous systems," *Proc. Amer. Control Conf.*, vol. 4, Jun. 1997, pp. 2513–2514.

[37] Y. Feng, X. Yu, and Z. Man, "Non-singular terminal sliding mode control of rigid manipulators," *Automatica*, vol. 38, no. 12, pp. 2159–2167, Dec. 2002.

CHENG ZHANG received the master's degree in mechanical principles from the Hubei University of Technology, China, in 2012. He is currently a Lecturer with the Hubei University of Technology. His research interests include intelligent manufacturing, inertial navigation, and flight control.

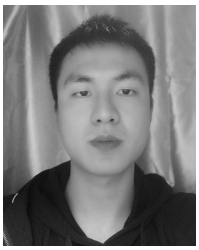

TIANLONG CHEN is currently pursuing the B.Eng. degree with the Hubei University of Technology (HBUT), Wuhan. With the help of Dr. Wei Shang, he has completed a few projects in the fields of formation control, stability analysis, and visual processing. His research interests include nonlinear control systems, nested adaptive, and trajectory tracking.

WEI SHANG received the Ph.D. degree in aeronautical and astronautical science and technology from the Beijing Institute of Technology, China, in 2017. He is currently a Lecturer with the Hubei University of Technology. His research interests include control theory of multi-agent systems and flight control.

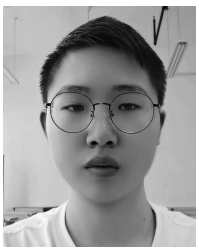

ZHONGZHONG ZHENG is currently pursuing the B.E. degree with the Hubei University of Technology (HBUT), Wuhan. He is also doing his research under Dr. Wei Shang. He helped to complete lots of jobs of quadrotor, which include distributed control, nested adaptive, and trajectory tracking.

HUIZHENG YUAN received the master's degree in instrument science and technology from the Beijing University of Aeronautics and Astronautics, China, in 2011. He is currently a Senior Engineer with the Hubei University of Technology. His research interests include inertial navigation, flight control, and intelligent manufacturing.